Research paper

A comparison of elasto-plastic parameters of S355 steel obtained in tensile tests using an extensometer, a strain gauge and an ARAMIS 3D DIC system

Marcin Chybiński[1], Janusz Dębiński[2], Adam Glema[3], Justyna Grzymisławska[4], Dariusz Jezierski[5], Łukasz Polus[6], Wojciech Szymkuć[7]

Abstract: The paper presents a comparison of three strain measurement methods. The mechanical parameters of S355 grade steel (yield strength, tensile strength, modulus of elasticity) were determined in tensile tests. Strains were measured using high resolution measuring instruments: an extensometer, a strain gauge and an ARAMIS 3D DIC system. In this paper, these three instruments have been used simultaneously in tensile tests for the first time. The results indicate that the values of the Young's modulus obtained using different techniques were similar when each instrument measured strain on the same side of the sample. Small differences were connected with different gauge lengths and their locations. The values of the Young's modulus determined on the opposite sides of the samples were more varied even when the same method was used (strain gauge measurements). For this reason, it is recommended to use double-sided averaging instruments when the Young's modulus is determined. The strain-curves obtained from the strain gauge measurements were incomplete and they came to an end at the end of the yield plateau due to the fact that they were damaged when the values of strain were relatively high. The extensometer was used up to the point where the strain reached 0.3% and then the strain was measured based on the distance between the machine clamps. The stress-strain curves

[1]Ph.D., Eng., Poznan University of Technology, Faculty of Civil and Transport Engineering, Piotrowo 5 Street, 60-965 Poznan, Poland, e-mail: marcin.chybinski@put.poznan.pl, ORCID: 0000-0003-2539-7764

[2]Ph.D., Eng., Poznan University of Technology, Faculty of Civil and Transport Engineering, Piotrowo 5 Street, 60-965 Poznan, Poland, e-mail: janusz.debinski@put.poznan.pl, ORCID: 0000-0003-1339-8698

[3]DSc., Ph.D., Eng., Poznan University of Technology, Faculty of Civil and Transport Engineering, Piotrowo 5 Street, 60-965 Poznan, Poland, e-mail: adam.glema@put.poznan.pl, ORCID: 0000-0001-7397-0137

[4]Ph.D., Eng., Poznan University of Technology, Faculty of Civil and Transport Engineering, Piotrowo 5 Street, 60-965 Poznan, Poland, e-mail: justyna.grzymislawska@put.poznan.pl, ORCID: 0000-0002-8129-3997

[5]Poznan University of Technology, Faculty of Civil and Transport Engineering, Piotrowo 5 Street, 60-965 Poznan, Poland, e-mail: dariusz.jezierski@put.poznan.pl, ORCID: 0000-0001-7326-3678

[6]Ph.D., Eng., Poznan University of Technology, Faculty of Civil and Transport Engineering, Piotrowo 5 Street, 60-965 Poznan, Poland, e-mail: lukasz.polus@put.poznan.pl, ORCID: 0000-0002-1005-9239

[7]M.Sc., Eng., Poznan University of Technology, Faculty of Civil and Transport Engineering, Piotrowo 5 Street, 60-965 Poznan, Poland, e-mail: wojciech.szymkuc@put.poznan.pl, ORCID: 0000-0002-8058-9825

obtained from the DIC system were complete because the system was able to monitor the sample until the very end of the tests.

1. Introduction

Tensile tests are used to determine the basic mechanical parameters of metals such as modulus of elasticity, yield strength, ultimate strength or elongation [1]. The results of tensile tests depend on many factors. Most importantly, they depend on the strain rate [2]. For this reason, material behaviour can be evaluated under low or high strain rate loading. Furthermore, they depend on test temperature. In particular, the mechanical parameters of metals are different at fire temperature and at room temperature [3, 4]. What is more, the method of sample preparation also has an impact on material parameters obtained from tensile tests. To limit the impact of heat on the strength parameters of metals, water or laser cutting may be used instead of torch cutting. Samples should be tested without additional layers, such as paint or galvanized layers. The surface of the samples should be perfectly smooth. Moreover, the size of a sample may also have an impact on the test results. Samples for tensile tests can be either flat or round. Sometimes, when they are too short it is difficult to properly fix them in the clamps of the testing machine and some slip may occur during the initial part of the stress-strain curve. For this reason, they are often long (e.g., 300 mm long). However, occasionally it is impossible to take relatively long samples from the structures because this could weaken them. In this situation, it is possible to take small samples from the construction, e.g., 20 mm long [5] or to use non-destructive methods, in which hardness is measured [6]. Last but not least, the results may depend on the measurement technique. A modulus of elasticity is one of the most difficult mechanical parameters to determine. To measure its value, high resolution measuring equipment must be used. In this paper, three strain measurement methods were used, i.e., an extensometer measurement, a strain gauge measurement and a Digital Image Correlation (DIC) method.

Contact clip-on extensometers are often used for strain measurement during tensile tests of steel. They are attached to samples without the use of glue, contrary to strain gauges, which require the use of glue. Extensometers can be used repeatedly in contrast to strain gauges. However, their initial gauge length is usually set, and their travel distance is relatively short. For this reason, they may be applied only to small samples, and they measure strain on gauge length only in one direction.

Electrical resistance strain gauges enable accurate measurement even on small or curved surfaces [7]. They have to be in contact with the measured object. A special glue has to be used to fix them. Furthermore, temperature compensation has to be used to compensate the effects caused by temperature.

Digital Image Correlation (DIC) method is a modern measurement technique which does not require direct contact with the tested object [7]. Displacements are determined based on the comparison of the captured digitized images [8]. Furthermore, the tested object is observed from a distance, which is important in case of samples expected to

fail suddenly [9]. What is more, the system allows for a more advanced analysis, such as, e.g., a heterogeneity analysis of the tested specimen [10]. For these reasons, it provides an alternative to traditional methods, such as an extensometer measurement and a strain gauge measurement. DIC relies on comparing digital photographs of a test piece at different deformation stages [11]. The system tracks block of pixels and measures surface displacement which may result in strain maps. The test piece is photographed using two digital cameras which are placed on one tripod. The system recognises the surface of the test piece area in the photographs. In many cases, the surface of the tested object has to be prepared in a special way for DIC to work effectively. The speckle pattern is often made by spraying black dots on the white background [12]. The pixel blocks should be random and diverse. The first image in the series is taken before loading and is treated as a reference photo [13]. The system creates a grid on the first image which consists of small rectangular planes called facets. Each facet has a single and unique texture of grey dots. For this reason, facets can be easily found in subsequent photos and compared to calculate the strain [14]. The facet density has an influence on the results, i.e., for larger facets deformation photos are less detailed [15]. The system uses efficient software techniques, which makes it possible to obtain sub-pixel resolutions and to take high resolution measurements [11]. Photographs may be obtained from digital cameras, high-speed video or microscopes. In this study, the ARAMIS DIC system is used. It is compatible with strength testing machines, which makes it possible to accurately correlate strain and stress in the tested piece [16]. The system is increasingly more popular because of its accuracy and non-contact operation. For example, it has been used to measure the displacement and deformation of LVL beams [17], high-strength fibre-reinforced concrete plates [18], thin-walled sigma-type steel beams with CFRP tapes [19], a steel beam [7], reactive powder concrete beams [20], thin-walled composite structures with central cut-out [21], and external facing of a sandwich panel [22]. The DIC method has increasingly more applications in many industries. For example, it is used to control the quality of products by comparing measurements with a reference model. It can be used to measure dynamic processes, e.g., in crash tests or crack propagation tests, when high-speed cameras are used. DIC used in combination with civil engineering surveying techniques can provide suitably accurate measurements of structures placed outdoors. Anomalies can be easily identified by comparing the captured images. The DIC system can be a component of a complex monitoring system. For example, this technique was successfully applied to measure displacements of a railway bridge in Nieporet (Poland) [23]. Unfortunately, DIC also has some limitations. The system needs efficient and fast big memory computers. The DIC method requires the laboratory personnel to be better prepared than in the case of extensometer and strain gauge measurements because the measuring surface of the sample has to be properly prepared and the device has to be calibrated [24]. What is more, when the relatively thin surface is analysed, the system has a problem with recognizing the tested surface. Last but not least, the measurement results may contain inaccuracies, which depend on the size of the tested area, software inaccuracies, lighting conditions (they should be the same throughout the test), the angle between the digital cameras and the tested piece, lens quality, surface preparation and camera noises [15]. The measurement inaccuracies can be determined using

the method presented by [25]. It is based on recording measurement noise. Many photos of an unloaded sample are taken. Each change observed between images is classified as a measurement noise.

The results of the DIC system measurements were compared with the values measured using strain gauges in [26]. The strain values obtained from strain gauges and based on the DIC system were in good agreement. Kowalewski et al. compared the stress-strain curves of 40H steel obtained using the DIC system and the extensometer [24]. The curves were almost identical with the necking region. The differences in yield strength, tensile strength and modulus of elasticity obtained using two different methods were 0.8%, 0.7% and 1.3%, respectively.

As presented above, the results obtained from the DIC systems were compared with the results of the strain gauge measurements and extensometer measurements in separate tests. In this paper, these three instruments have been used simultaneously in tensile tests for the first time. The main goal of this paper is to compare the moduli of elasticity and the stress-strain curves determined using three different methods.

2. Laboratory tests

The uniaxial tensile tests of steel were carried out using an Instron Satec testing machine (Instron, Grove City, PA) with a maximum capacity of 300 kN. The laboratory tests were conducted at room temperature, taking into account the rules presented in the PN-EN ISO 6892-1 standard [27]. The Young's modulus, the yield strength and the ultimate strength of the S355 steel were determined. The tensile tests were carried out using flat samples.

First, the $70 \times 240 \times 320$ mm plate was cut from the $70 \times 2000 \times 12000$ mm plate. The 70 mm steel plate was in the grade and delivery condition S355J2+N according to standard EN 10025-2 [28]. The information about the steel plate, presented below, was obtained from the manufacturer's inspection certificate [29]. For the test temperature of 20°C, the yield strength of steel (R_{eH}) was 409 MPa, the tensile strength of steel (R_m) was 577 MPa, and the elongation after fracture of steel (A_5) was = 31.9%. The plate was also tested in an impact test at 20°C, and the mean impact energy was 200 J. Furthermore, a bending test of weldability was carried out for the plate according to ABV/SEP 1390 [30], using manual arc welding and a welding electrode ER 146 (E 38 0 RC 11) with a diameter of 5 mm and a length of 450 mm [31]. The result of this test was positive. What is more, a tensile test was carried out in the direction perpendicular to the surface, to obtain the mechanical properties through the thickness of the product, i.e., "Z" test. The plate was of Z35 quality class, and the mean value of the transverse reduction of the area in the tensile test was 64.8%. Moreover, ultrasonic tests showed no internal discontinuities for quality class S1E1 according to the standard PN-EN 10160 [32]. The chemical composition of the steel based on [29] is shown in Table 1. The carbon equivalent (CEV) was 0.45.

Rectangular 5 mm and 16 mm plates were cut out from the hot rolled steel plate ($70 \times 240 \times 320$ mm) described above, using water cutting to limit the influence of heat on the strength parameters of steel (Figure 1). The plates were cut out from the same 70 mm

Table 1. Chemical composition of S355 steel [29]

C [%]	Mn [%]	Si [%]	P [%]	S [%]	Cu [%]	Ni [%]
0.190	1.510	0.400	0.020	0.003	0.016	0.053
Cr [%]	Mo [%]	V [%]	Ti [%]	Al [%]	N [%]	Nb [%]
0.027	0.005	0.009	0.002	0.032	0.007	0.005

plate to make sure they were all made of the same steel. Next, flat samples were cut out from these 5 mm and 16 mm plates using water cutting. Each sample was prepared in accordance with the rules presented in the standard [27] and proportional test specimens were used.
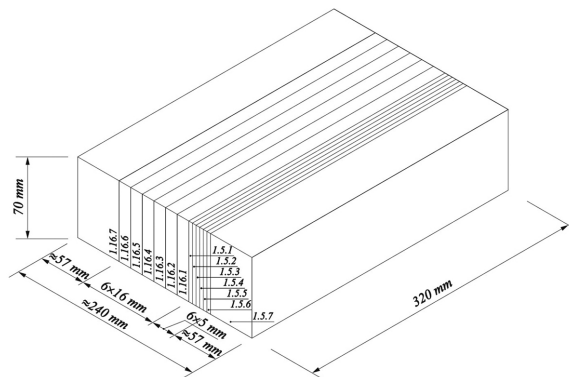
Fig. 1. The hot rolled steel plate ($70 \times 240 \times 320$ mm)

The cross-section areas of the samples were the same (5×16 mm). However, the geometry of the 5 mm and 16 mm samples was different (Figure 2). Due to the fact that the samples had two types of geometry, different variants of instruments configurations could be used. What is more, the samples were made of the same steel, and they had the same cross-sections, and therefore they were comparable. In the tensile tests, the tensile direction was parallel to the rolling direction of the hot rolled steel plate (direction 1).

The initial stress rate $\dot{R}$ of 6.0 MPa/s was used up to 0.2% of the nominal elongation (in the elastic range). In the plastic range, the speed of the movement of the testing machine traverse was 0.5 mm/s. Three different methods were used to measure strains in the elastic range of tests:
– an contact clip-on extensometer (Instron, HighWycombe, Buckinghamshire, UK) with a 50 mm gauge and a travel range of –2.5 mm to +25.0 mm,
– two strain gauges (Hottinger, Darmstadt, Germany) with a 10 mm gauge, 0.2% transverse sensitivity, and 120 Ω ±0.35% resistance.
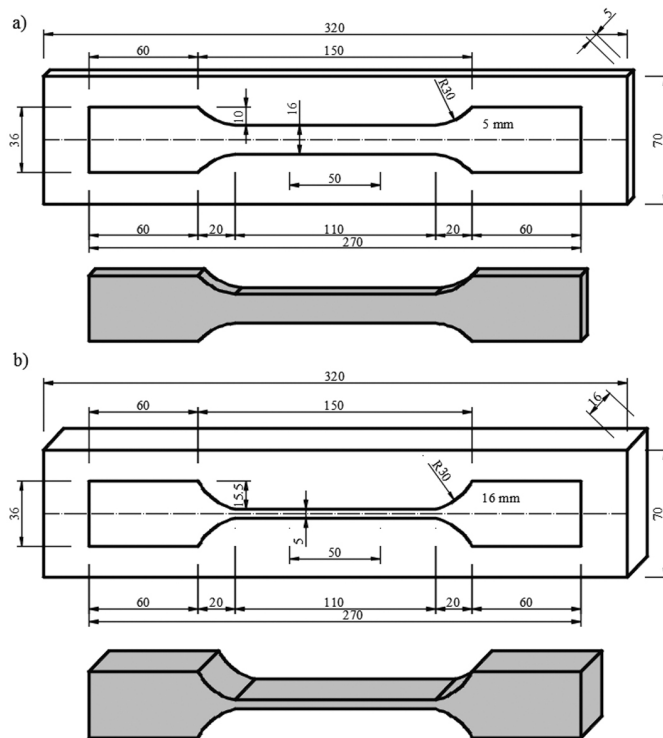– an ARAMIS 3D Camera 6M system (GOM GmbH, Braunschweig, Germany).
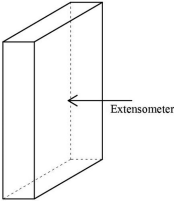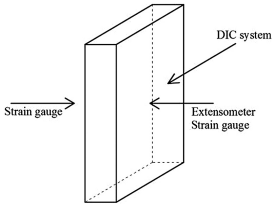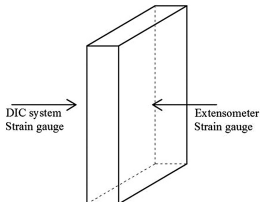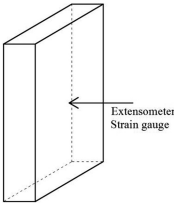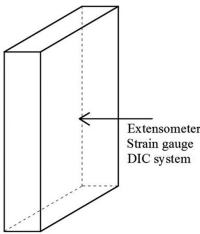
Fig. 2. The flat samples: a) 5 mm, b) 16 mm

The names of the specimens contain information on 4 parameters: D.T.N.V. D represents the direction of the sample: 1 – the length of the sample parallel to the rolling direction of the hot rolled steel plate, 2 – the length of the sample perpendicular to the rolling direction of the hot rolled steel plate, 3 – the length of the sample at an angle of 45 degrees to the rolling direction of the hot rolled steel plate. The present article presents the results for direction 1 only. T is the thickness of the sample, N is the number of the specimen in a given variant of thickness, and V is a variant of instruments configuration. The instruments were placed on the specimens with different configurations (Table 2).

In variant A, only the extensometer was used. In variant B, strain was measured on three sides of the specimen (Figure 3). The extensometer and the first strain gauge measured strain on one side of the sample, the second strain gauge measured strain on the opposite side of the sample, and the DIC system measured strain on the edge of the sample (Figure 3).

In variant C, the DIC system and the first strain gauge measured strain on one side of the sample, and the extensometer and the second strain gauge measured strain on the opposite side of the sample (Figure 4).

In variant D, the extensometer and the strain gauge measured strain on one side of the sample. In variant E, the DIC system, the extensometer and the strain gauge measured strain on the same side of the sample (Figure 5).

Table 2. The variants of instruments configuration

Sample	Variant	Instruments configuration
1.5.1.A	A	Extensometer
1.5.2.B	B	DIC system / Strain gauge / Extensometer Strain gauge
1.5.3.C, 1.16.3.C	C	DIC system Strain gauge / Extensometer Strain gauge
1.16.1.D, 1.16.4.D	D	Extensometer Strain gauge
1.16.2.E	E	Extensometer Strain gauge DIC system

The DIC system made it possible to measure deformation without contact. The measuring volume with a range of $160 \times 135 \times 90$ mm was used. On the surface of each specimen, a special pattern comprising black spots on a white mat paint background was crated (Figure 6).
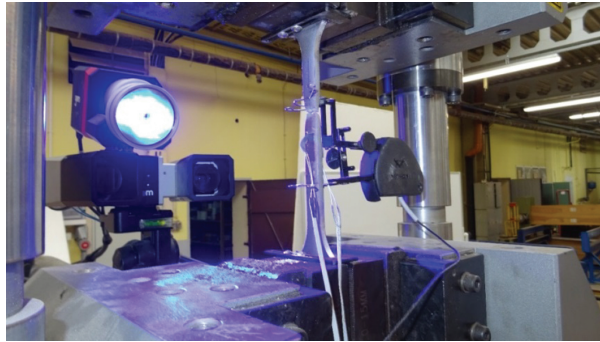
Fig. 3. Variant B of instruments configuration (5 mm sample)
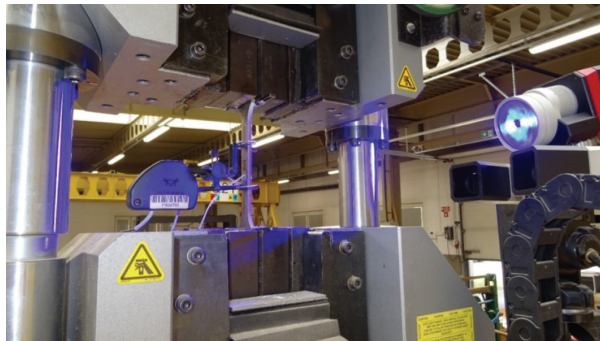
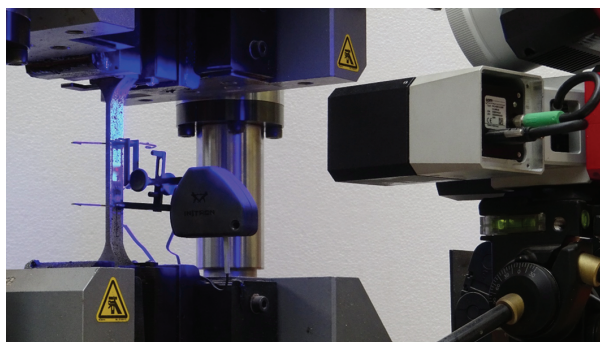Fig. 4. Variant C of instruments configuration (5 mm sample)

Fig. 5. Variant E of instruments configuration (16 mm sample)

The DIC system was calibrated before the tests and it recognised the surface of the specimens. At the beginning of the measurement, an undistorted image of the analysed surface was taken, and then a series of photographs corresponding to the next load stages were taken. Pixels in the photographs had their coordinates [33]. 21 pixels was chosen
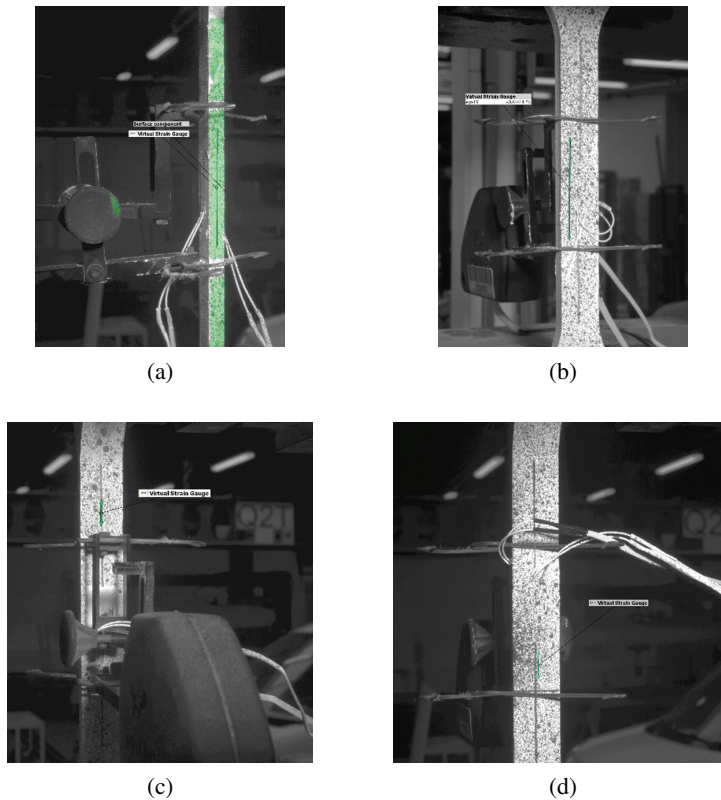
Fig. 6. Virtual strain gauges used for: a) 1.5.2.B specimen, b) 1.5.3.C specimen,
c) 1.16.2.E specimen, d) 1.16.3.C specimen

as the facet size, and the distance between the centre points of individual facets (point distance) was 16 pixels. Thanks to the use of two cameras and the unique pattern on the specimen surface, the software was able to find facets in the images from two cameras and compute the distances between the points. The unique pattern of the black spots allowed for creating a virtual extensometer for each test (Figure 6). The photos were taken at a 5 Hz frequency, allowing for strain computation during the whole tensile test, with a frequency large enough to capture the yield plateau. After completing the test, the photographs taken by digital cameras were analysed using the GOM Correlate 2020 software based on the digital image correlation and point tracking algorithms for 3D testing data. Each photograph was compared with the initial photograph. In the software, the user may create displacement values of selected points [34]. Strain was determined with the optical measurement technique only on the surface of the samples. The gauge length of the DIC system was determined after the tests. The use of a non-contact measuring system usually allows to measure the displacement over the entire sample surface [35]. However, in this article, the gauge length of the system was limited by the knife edges and the arms of

the extensometer used as a second device. The following gauge lengths of the DIC system were used for the specimens: 40 mm (1.5.2.B and 1.5.3.C specimen) and 10 mm (1.16.2.E and 1.16.3.C specimen).

The modulus of elasticity was determined in accordance with Annex G from [27]. In this document, it was recommended to measure strain on the opposite sides of the test specimen and to use the extensometer gauge length of at least 50 mm. The average strain, necessary for the determination of the modulus of elasticity, should be calculated for each value of stress by averaging the strain from the opposite sides of the test specimen. In this paper, the modulus of elasticity was first calculated for each instrument separately and then as a mean value based on the strain measured from the opposite sides of the test specimen. Straight lines were determined between a lower stress value and an upper stress value.

3. The results of the laboratory tests

The mechanical parameters of steel obtained from the uniaxial tensile tests are presented in Table 3.

Table 3. Mechanical parameters of steel

Sample	R_{eL} [MPa]	R_{eH} [MPa]	R_m [MPa]	E_e [GPa]	E_{sg1} [GPa]	E_{sg2} [GPa]	E_{DIC} [GPa]	$\frac{E_{sg1}+E_{sg2}}{2}$ [GPa]	$\frac{E_e+E_{DIC}}{2}$ [GPa]
1.5.1.A	341.27	349.25	531.83	–	–	–	–	–	–
1.5.2.B	349.24	349.97	534.54	184.9	208.8	201.9	154.4	205.4	–
1.5.3.C	343.92	345.77	529.29	183.2	205.9	205.7	179.8	205.8	181.5
1.16.1.D	332.30	341.09	523.98	188.2	193.8	–	–	–	–
1.16.2.E	336.41	344.70	528.37	182.5	187.4	–	202.6	–	–
1.16.3.C	342.56	349.26	532.41	193.4	209.3	199.1	215.2	204.2	204.3
1.16.4.D	350.60	353.65	540.08	191.0	–	203.0	–	–	–

R_{eL} – lower yield strength
R_{eH} – upper yield strength
R_m – tensile strength
E_e – modulus of elasticity determined using an extensometer
E_{sg1} – modulus of elasticity determined using strain gauge 1
E_{sg2} – modulus of elasticity determined using strain gauge 2
E_{DIC} – modulus of elasticity determined using the DIC system

Stress-strain curves and straight lines determined between a lower stress value and an upper stress value are demonstrated in Figures 7–19. One can observe that the analysed steel displayed yield-point runout and had two yield points (upper and lower) typical for low-carbon steel (Figure 7).
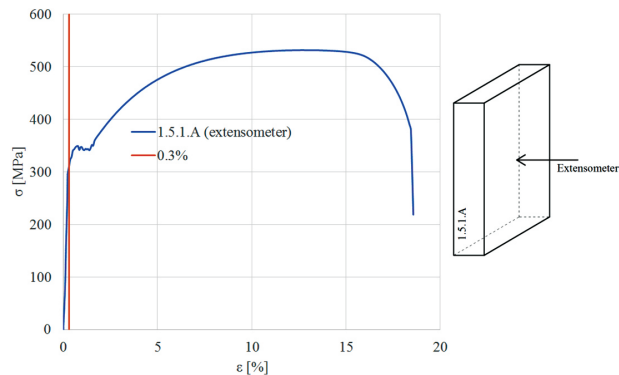
Fig. 7. Stress-strain curves for sample 1.5.1.A

The stress-strain curves based on the measurements using the strain gauge, the extensometer and the DIC system were similar. However, small differences were visible. Figure 8 presents the stress-strain curves for sample 1.5.2.B. The strain was measured on three sides of this specimen. One can observe that the 1.5.2.B (extensometer) curve is consistent with the remaining curves but only at low strain values (<0.3%). For higher strain values the difference between the blue curve and the remaining curves is visible.
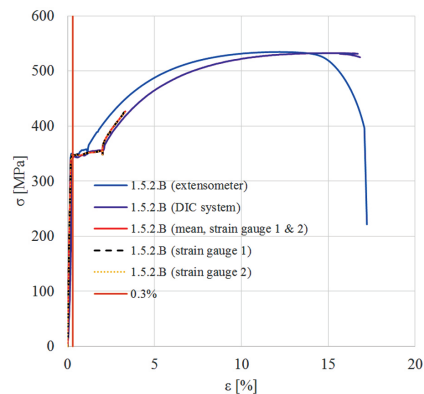
Fig. 8. Stress-strain curves for sample 1.5.2.B

This phenomenon is connected with the fact that the extensometer was used only up to the point where the strain reached 0.3% and then its value was measured based on the distance between the machine clamps. The extensometer was unfastened from the sample to avoid its damage. In the plastic range of the test, strain was measured taking into account the longer gauge length (150 mm). The gauge lengths for the remaining instruments (10 mm, 40 mm) were much smaller than the gauge length between the clamps of the testing machine (150 mm). As a result, the values of strain for the same level of stress were lower for the blue curve. For this reason the blue stress-strain curve had a shorter yield plateau.

Figure 9 demonstrates that the values of the Young's modulus obtained on different sides of the sample were different mainly due to the fact that it was difficult to ensure the optimal conditions for tensile tests such as the perfect alignment and smoothness of the test specimen surface. For this reason, it is important to calculate the modulus of elasticity based on the mean value of the strains measured on the opposite sides of the test specimen.
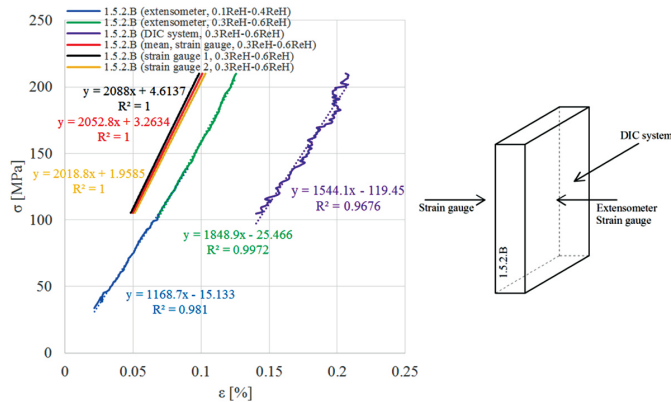

Fig. 9. The straight lines determined between 10% of R_{eH} and 40% of R_{eH}, and between 30% of R_{eH} and 60% of R_{eH} with the coefficient of determination R^2 for sample 1.5.2.B, and the instrument configuration

The stress-strain curve obtained from the measurement using the strain gauge was not full because the strain gauge was damaged when the strain reached a high value (about 3%) (Figure 10).
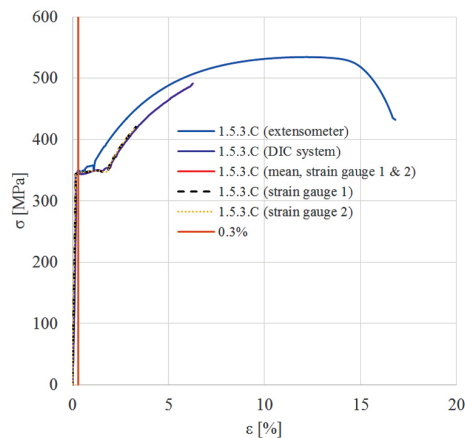
Fig. 10. Stress-strain curves for sample 1.5.3.C

Furthermore, the transverse sensitivity of the strain gauges used in this study was 0.2%. For the longitudinal strain equal to 3% the transverse strain was 0.9% for Poisson's ratio

(ν) of 0.3. For such a high transverse strain (> 0.2%), the results of the strain gauge measurements may contain inaccuracies connected with the transverse error.

Figure 11 demonstrates that the value of the Young's modulus depends not only on the side of the sample but also on the gauge length and on the location of the gauge on the side. The extensometer and one of the strain gauges measured strain on the same side of the sample. However, the values of the Young's modulus obtained using these two methods were quite different.
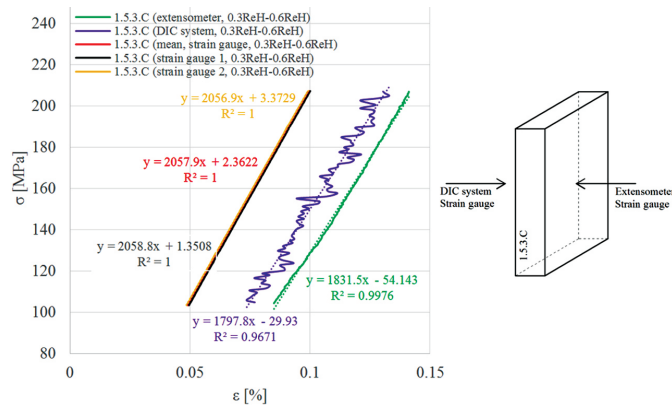
Fig. 11. The straight lines determined between between 30% of R_{eH} and 60% of R_{eH} with the coefficient of determination R^2 for sample 1.5.3.C, and the instrument configuration

Figures 12– 19 present stress-strain curves for the remaining samples.
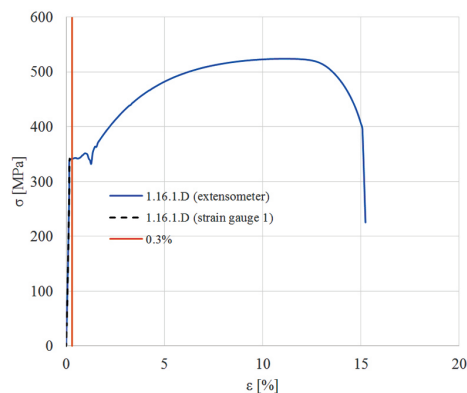

Fig. 12. Stress-strain curves for sample 1.16.1.D

Figure 17 demonstrates how important it is to calculate the modulus of elasticity based on the mean value of strain measured on the opposite sides of the test specimen. The DIC system and the first strain gauge measured strain on one side of the sample, while the extensometer and the second strain gauge measured strain on the opposite side of the
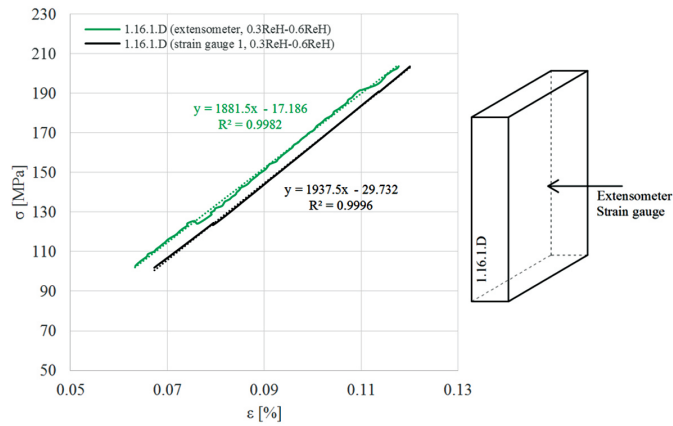
Fig. 13. The straight lines determined between 30% of R_{eH} and 60% of R_{eH} with the coefficient of determination R^2 for sample 1.16.1.D, and the instrument configuration
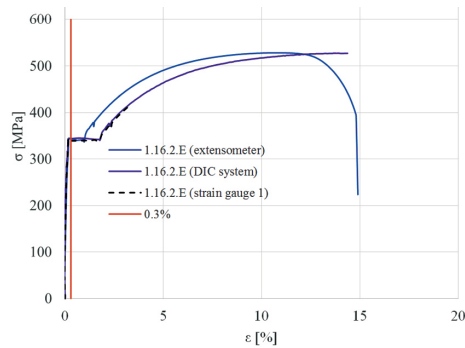

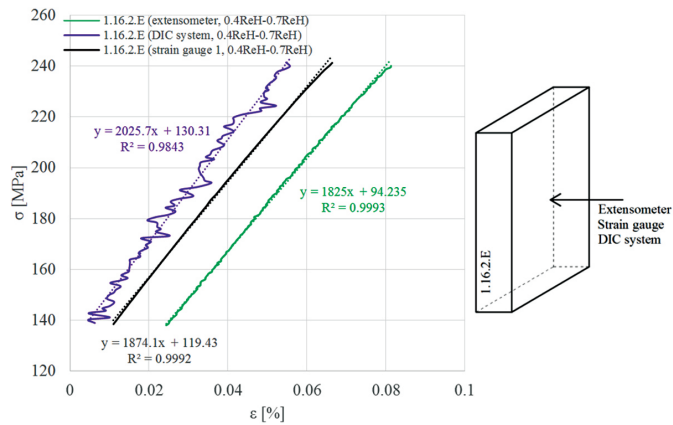Fig. 14. Stress-strain curves for sample 1.16.2.E

Fig. 15. The straight lines determined between 40% of R_{eH} and 70% of R_{eH} with the coefficient of determination R^2 for sample 1.16.2.E, and the instrument configuration
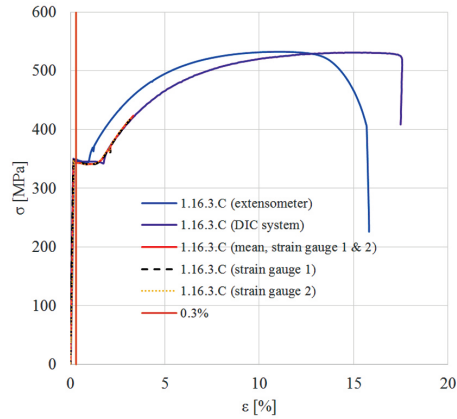
Fig. 16. Stress-strain curves for sample 1.16.3.C

Fig. 17. The straight lines determined between 30% of R_{eH} and 60% of R_{eH} with the coefficient of determination R^2 for sample 1.16.3.C, and the instrument configuration
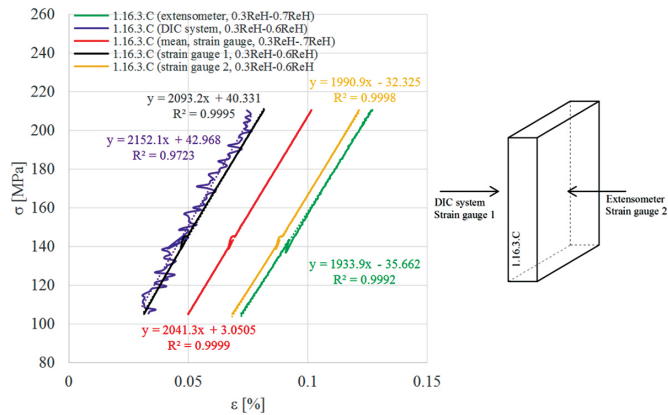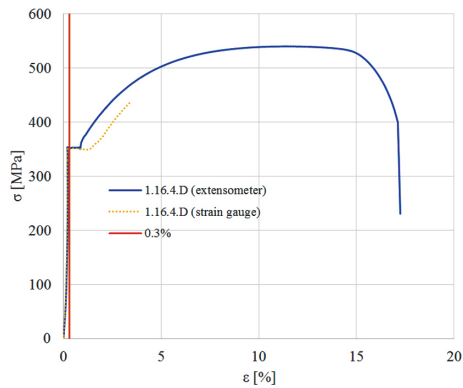

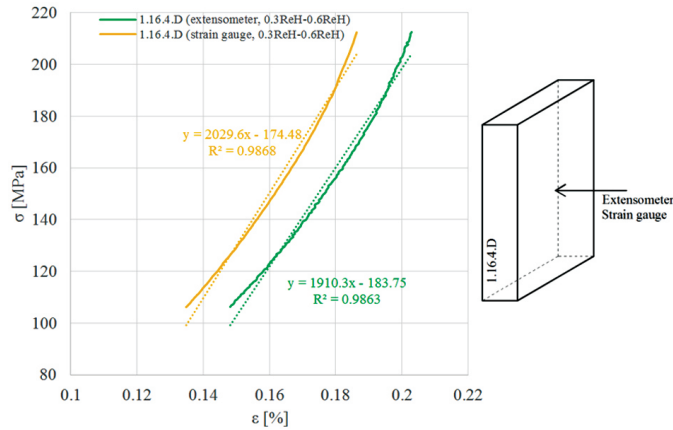Fig. 18. Stress-strain curves for sample 1.16.4.D

Fig. 19. The straight lines determined between 30% of R_{eH} and 60% of R_{eH} with the coefficient of determination R^2 for sample 1.16.4.D, and the instrument configuration

sample. The modulus of elasticity determined using the DIC system (215.2 GPa) was only 1.03 times higher than the one determined using the first strain gauge (209.3 GPa). The modulus of elasticity determined using the extensometer (193.4 GPa) was only 1.03 times lower than the one determined using the second strain gauge (199.1 GPa). The mean value of the modulus of elasticity determined using the strain gauges (204.2 GPa) was almost the same as the mean value of the modulus of elasticity determined using the extensometer and the DIC system (204.3 GPa).

4. Conclusions

Thanks to use of high-resolution measuring equipment, it was possible to determine the Young's modulus of S355 steel. The values of the Young's modulus obtained using three different techniques were similar. Small differences were connected with different gauge lengths and their locations. The values of the Young's modulus obtained on different sides of the sample were different mainly due to the fact that was difficult to ensure the optimal conditions for tensile tests such the perfect alignment and smoothness of the test specimen surface. For this reason, it is important to calculate the modulus of elasticity based on the mean value of the strains measured on the opposite sides of the test specimen. The value of the Young's modulus depends not only on the sample side but also on the gauge length and on the location of the gauge on the side. The strain gauge worked only up to the point where the strain reached 3%. Then they were damaged and stopped taking measurements. For this reason, the strain-curves obtained from the strain gauge measurements were incomplete. The extensometer was used only up to the point where the strain reached 0.3% to avoid its damage. In the plastic range of the test, the strain was calculated based on the measurements of the distance between the machine clamps. For this reason, the stress-strain curve based

on the longer gauge length had a shorter yield plateau. The strain-curves obtained from the DIC system were complete because the system was able to monitor the sample until the end of the tests. For this reason, DIC is an effective technique for determining the mechanical parameters of steel based on a tensile test. However, it also has some limitations. In this article, the gauge length of the DIC system was limited by the knife edges and the arms of the extensometer used as a second device. Last but not least, the results for a relatively low strain contained camera noises.

References

[1] J. Dębiński, J. Grzymisławska, *Ćwiczenia laboratoryjne z wytrzymałości materiałów*. Poznań: Wydawnictwo Politechniki Poznańskiej, 2016.

[2] M. Chybiński, Ł. Polus, M. Ratajczak, P.W. Sielicki, "The evaluation of the fracture surface in the AW-6060 T6 aluminium alloy under a wide range of loads", *Metals*, 2019, vol. 9, no. 3, art. ID 9030324; DOI: 10.3390/met9030324.

[3] M. Malendowski, A. Glema, W. Szymkuc, "Performance based coupled CFD-FEM analysis of 3-bay high industrial hall under natural fire", in: *Application of Structural Fire Engineering*, F. Wald, et al., Eds. Czech Technical University in Prague, 2017; DOI: 10.14311/asfe.2015.014.

[4] M. Chybiński, Ł. Polus, "Bending resistance of metal-concrete composite beams in a natural fire", *Civil and Environmental Engineering Reports*, 2018, vol. 28, no. 4, pp. 149–162; DOI: 10.2478/ceer-2018-0058.

[5] M. Chybiński, Z. Kurzawa, Ł. Polus, "Problems with buildings lacking basic design documentation", *Procedia Engineering*, 2017, vol. 195, pp. 24–31.

[6] M. Szumigała, M. Chybiński, Ł. Polus, "Określanie parametrów wytrzymałościowych stali w istniejących konstrukcjach", *Materiały Budowlane*, 2016, no. 11, pp. 78–79.

[7] P. Szewczyk, P. Kudyba, "Effectiveness of selected strain and displacement measurement techniques in Civil Engineering", *Buildings*, 2022, vol. 12, no. 2, art. ID 172; DOI: 10.3390/buildings12020172.

[8] T. Gajewski, T. Garbowski, "Calibration of concrete parameters based on digital image correlation and inverse analysis", *Archives of Civil and Mechanical Engineering*, 2014, vol. 14, no. 1, pp. 170–180; DOI: 10.1016/j.acme.2013.05.012.

[9] Ł. Krawczyk, M. Gołdyn, T. Urban, "Digital image correlation systems in the experimental investigations: capabilities and limitations", *Archives of Civil Engineering*, 2019, vol. 65, no. 1, pp. 171–180; DOI: 10.2478/ace-2019-0012.

[10] M. Chuda-Kowalska, "Effect of foam's heterogeneity on the behaviour of sandwich panels", *Civil and Environmental Engineering Reports*, 2019, vol. 29, no. 4, pp. 97–111; DOI: 10.2478/ceer-2019-0047.

[11] N. McCormick, J. Lord, "Digital Image Correlation", *Materials Today*, 2010, vol. 13, no. 12, pp. 52–54; DOI: 10.1016/S1369-7021(10)70235-2.

[12] J. Górszczyk, K. Malicki, T. Zych, "Application of Digital Image Correlation (DIC) method for road material testing", *Materials*, 2019, vol. 12, no. 15, art. ID 2349; DOI: 10.3390/ma12152349.

[13] B. Goszczyńska, W. Trąmpczyński, J. Tworzewska, "Analysis of crack width development in reinforced concrete beams", *Materials*, 2021, vol. 14, no. 11, art. ID 3043; DOI: 10.3390/ma14113043.

[14] K. Urbańska, "Zastosowanie systemu Aramis do pomiarów odkształceń konstrukcji murowych", *Zeszyty Naukowe Uniwersytetu Zielonogórskiego, Inżynieria Środowiska*, 2017, no. 46, pp. 48–59.

[15] Ł. Krawczyk, M. Gołdyn, T. Urban, "O niedokładnościach systemów cyfrowej korelacji obrazu", *Journal of Civil Engineering, Environment and Architecture*, 2017, vol. 34, no. 64, pp. 259–270; DOI: 10.7862/rb.2017.120.

[16] K. Walotek, J. Bzówska, A. Ciołczyk, "Influence of addition of shredded rubber waste on deformability of binder-bound anthropogenic material mixtures", *Archives of Civil Engineering*, 2021, vol. 67, no. 4, pp. 207–223; DOI: 10.24425/ace.2021.138495.

[17] M.M. Bakalarz, P.G. Kossakowski, P. Tworzewski, "Strengthening of bent LVL beams with near-surface mounted (NSM) FRP reinforcement", *Materials*, 2020, vol. 13, no. 10, art. ID 2350; DOI: 10.3390/ma13102350.

[18] P. Smarzewski, M. Szwaj, A. Szewczak, "Analizy stanów deformacji zginanych płyt z betonu i fibrobetonu wysokowartościowego", *Budownictwo i Architektura*, 2012, vol. 10, pp. 37–52.

[19] I. Szewczak, P. Rozylo, M. Snela, K. Rzeszut, "Impact of adhesive layer thickness on the behavior of reinforcing thin-walled sigma-type steel beams with CFRP tapes", *Materials*, 2022, vol. 15, no. 3, art. ID 1250; DOI: 10.3390/ma15031250.

[20] A. Denisiewicz, M. Kuczma, "Two-Scale Modelling of Reactive Powder Concrete. Part III: Experimental Tests and Validation", *Engineering Transactions*, 2015, vol. 63, no. 1, pp. 55–76.

[21] P. Rozylo, K. Falkowicz, "Stability and failure analysis of compressed thin-walled composite structures with central cut-out, using three advanced independent damage models", *Composite Structures*, 2021, vol. 273, art. ID 114298; DOI: 10.1016/j.compstruct.2021.114298.

[22] R. Studziński, K. Ciesielczyk, "Connection stiffness between thin-walled beam and sandwich panel", *Journal of Sandwich Structures & Materials*, 2019, vol. 21, no. 6, pp. 2042–2056; DOI: 10.1177/1099636217750539.

[23] M. Malesa, D. Szczepanek, M. Kujawińska, A. Świercz, P. Kołakowski, "Monitoring of civil engineering structures using Digital Image Correlation technique", *EPJ Web of Conferences*, 2010, no. 6, art. ID 31014; DOI: 10.1051/epjconf/20100631014.

[24] Z.L. Kowalewski, L. Dietrich, M. Kopeć, T. Szymczak, P. Grzywna, "Nowoczesne systemy optyczne w badaniach mechanicznych – budowa, działanie, zastosowania", presented at XXII Seminarium Nieniszczące Badania Materiałów, Zakopane, 16-18 marca 2016.

[25] M. Kneć, "Technika cyfrowej korelacji obrazów w analizie deformacji połączeń elementów konstrukcji stosowanych w lotnictwie", Ph.D. Dissertation, Rzeszow University of Technology, Poland, 2015.

[26] M.R.L. Gower, R.M. Shaw, "Towards a Planar Cruciform Specimen for Biaxial Characterisation of Polymer Matrix Composites", *Applied Mechanics and Materials*, 2010, vol. 24-25, pp. 115–120; DOI: 10.4028/www.scientific.net/AMM.24-25.115.

[27] *PN-EN ISO 6892-1 Metallic materials – Tensile testing – Part 1: Method of test at room temperature*. Polish Committee for Standardization and European Committee for Standardization, Warsaw-Brussels, Poland-Belgium, 2020.

[28] *EN 10025-2 Hot rolled products of structural steels – Part 2: Technical delivery conditions for non-alloy structural steels*. European Committee for Standardization, Brussels, Belgium, 2019.

[29] Inspection certificate 3.1, Hot rolled steel plates in grade S355J2+N acc. to quality EN 10025-2, Vítkovice Steel, 2020.

[30] *ABV – SEP 1390.* 1996.

[31] *PN-EN ISO 2560:2021 Welding consumables. Covered electrodes for manual metal arc welding of non-alloy and fine grain steels – Classification*. Polish Committee for Standardization and European Committee for Standardization, Warsaw-Brussels, Poland-Belgium, 2021.

[32] *PN-EN 10160:2001, Ultrasonic testing of steel flat product of thickness equal or greater than 6 mm (reflection method)*. Polish Committee for Standardization and European Committee for Standardization, Warsaw-Brussels, Poland-Belgium, 2001.

[33] P. Smarzewski, "Processes of cracking and crushing in hybrid fibre reinforced high-performance concrete slabs", *Processes*, 2019, vol. 7, no. 1, art. ID 49; DOI: 10.3390/pr7010049.

[34] J. Wojciechowski, M.D. Gajewski, C.W. Ajdukiewicz, "Procedura wyznaczania parametrów sprężysto-plastyczności ze wzmocnieniem izotropowym na podstawie badań doświadczalnych przy zastosowaniu systemu optyczno-pomiarowego ARAMIS", in: *Deformacje i wytrzymałość materiałów i elementów konstrukcji*, S. Jemioło, A. Szwed, Eds. Warszawa: Wydział Inżynierii Lądowej Politechniki Warszawskiej, 2013, pp. 93-98.

[35] T. Garbowski, A. Knitter-Piątkowska, A. Marek, "New edge crush test configuration enhanced with full-field strain measurements", *Materials*, 2021, vol. 14, no. 19, art. ID 5768; DOI: 10.3390/ma14195768.

Porównanie parametrów sprężysto-plastycznych stali S355 w próbie rozciągania metodami pomiarowymi z użyciem ekstensometru, tensometru i systemu cyfrowej korelacji obrazu ARAMIS 3D

Słowa kluczowe: ARAMIS, mechaniczne parametry stali, moduł elastyczności, próba rozciągania, cyfrowa korelacja obrazu

Streszczenie:

W artykule przedstawiono porównanie trzech metod pomiarowych odkształceń. Autorzy wyznaczyli parametry mechaniczne stali S355 (granicę plastyczności, wytrzymałość na rozciąganie, moduł elastyczności) w próbie rozciągania. Odkształcenie zostało wyznaczone przy użyciu przyrządów pomiarowych o wysokiej rozdzielczości: ekstensometru, tensometru oraz systemu cyfrowej korelacji obrazu ARAMIS 3D. Po raz pierwszy w próbie rozciągania wykorzystano wszystkie urządzenia pomiarowe jednocześnie. Wartości modułu Younga wyznaczone za pomocą różnych metod były zbliżone, gdy urządzenie mierzyły odkształcenie po tej samej stronie próbki. Niewielkie różnice wynikały z różnych długości pomiarowych oraz z faktu, że przyrządy nie mierzyły odkształcenia dokładnie na tej samej bazie pomiarowej. Wartości moduły Younga wyznaczone dla przeciwnych stron próbki różniły się bardziej nawet, gdy zastosowano tą samą metodę pomiarową (pomiar odkształceń za pomocą tensometrów). W związku z tym w celu wyznaczenia prawidłowej wartości modułu elastyczności zaleca się stosowanie dwóch urządzeń rozmieszonych na przeciwnych stronach próbki oraz obliczanie modułu sprężystości na podstawie średniej wartości odkształcenia. Krzywe naprężenie-odkształcenie otrzymane z pomiarów tensometrycznych były niekompletne i kończyły się zaraz po półce plastycznej, ponieważ tensometry ulegały uszkodzeniu przy większych wartościach odkształceń. Ekstensometr był wykorzystywany do momentu, w którym odkształcenia osiągnęły wartość 0,3%. Od tej wartości odkształcenia były wyznaczane na podstawie odległości między szczękami maszyny. Krzywe naprężenie-odkształcenie otrzymane na podstawie cyfrowej korelacji obrazu były kompletne, ponieważ system mógł obserwować próbkę przez całe badanie. Z tego względu, metoda cyfrowej korelacji obrazu jest skutecznym narzędziem, które może być wykorzystane do wyznaczania parametrów mechanicznych stali.